applied sciences

MDPI

Article

# Research on Compression Behavior of Square Thin-Walled CFST Columns with Steel-Bar Stiffeners

**Zhao Yang** * and **Chengxiang Xu**

School of Urban Construction, Wuhan University of Science and Technology, Wuhan 430065, China; cx_xu@sina.com
* Correspondence: yangzhao@wust.edu.cn; Tel.:+86-027-68893651

Received: 6 August 2018; Accepted: 6 September 2018; Published: 10 September 2018

**Abstract:** Local buckling in steel tubes was observed to be capable of reducing the ultimate loads of thin-walled concrete-filled steel-tube (CFST) columns under axial compression. To strengthen the steel tubes, steel bars were proposed in this paper to be used as stiffeners fixed onto the tubes. Static-loading tests were conducted to study the compression behavior of square thin-walled CFST columns with steel bar stiffeners placed inside or outside the tube. The effect and feasibility of steel bar stiffeners were studied through the analysis of failure mode, load–displacement relationship, ultimate load, ductility, and local buckling. Different setting methods of steel bars were compared as well. The results showed that steel-bar stiffeners proposed in this paper can be effective in delaying local buckling as well as increasing the bearing capacity of the columns, but will decrease the ductility of the columns. In order to obtain a higher bearing capacity of columns, steel bars with low stiffness should be placed inside and steel bars with high stiffness should be placed outside of the steel tubes. The study is helpful in providing reference to the popularization and application of this new structural measure to avoid or delay the local buckling of thin-walled CFST columns.

**Keywords:** steel-bar stiffeners; square thin-walled CFST column; compression behavior; local buckling; structural measure

## 1. Introduction

Thin-walled concrete-filled steel-tube (CFST) columns have received extensive attention from scholars and engineers, because of their significant advantages to reduce the amount of steel consumption and workload of welding. Ahmad studied the local buckling restraining behavior of concrete-filled steel tubular columns under seismic loads and the interaction between steel tube and concrete was discussed [1]. Montuori et al. studied the evaluation of the ultimate behavior of concrete-filled tubular (CFT) members subjected to nonuniform bending moments and presented a fiber model able to predict the ultimate response of CFT members [2]. Elchalakani et al. presented a new method to determine new ductile slenderness limits suitable for plastic design of structures based on the measured strains in plastic-bending tests on concrete-filled tubes [3]. Choi et al. showed, through experimental and numerical investigations, that thick flanges of high-strength steel, thin webs of mild steel, and electrodes for the thin and mild steel can be used to increase cost efficiency without performance degradation and the hybrid rectangular CFT (RCFT) sections can develop full plastic strength [4]. Campiche et al. evaluated the seismic behavior of CFS buildings sheathed with gypsum panels by shaking-table tests and developed a numerical model able to simulate the dynamic/earthquake response in an OpenSees environment [5]. Ghazijahani et al. studied the structural behavior of timber-filled and carbon fiber reinforced polymer (CFRP) jacketed circular steel tubes and clarified the effect of each material on structural behavior [6]. Then, they studied the effect of timber cores on the structural response of concrete-filled circular tubes under compression [7]. Ding et al. established finite element models of concrete-filled steel-tube stub columns under local compression and proposed precise and concise formulas [8]. The steel tube can be used as the concrete formwork and support the stirrup inside as well. But, mechanical deficiencies still exist, so that local buckling is easy to form into the thin-walled steel tube, thus making it unable to completely use the bearing capacity of the core concrete inside the tube. Therefore, the improvement of local-buckling performance of the thin steel tube becomes a critical problem in the study of thin-walled CFST columns. Some experiments and analysis have been conducted to resolve the problem. Uy et al. used a finite strip model for elastic local buckling to study the behavior of steel plates in composite steel–concrete members, considered the buckling of the steel skin and suggested the width-to-thickness ratios suitable for design [9]. Schnabl et al. presented an efficient mathematical model for studying the global buckling behavior of CFST columns with compliant interfaces [10]. Thai et al. proposed a new stress-strain model considering the local-buckling effect [11]. Dundu conducted buckling tests of square concrete-filled steel tubes under concentric axial compression [12]. Long et al. studied the local-buckling behavior of eccentrically loaded rectangular CFT columns and derived the formulas for critical buckling stress of the steel plates [13]. Song et al. investigated factors that affect the buckling and postbuckling behavior of steel flanges of partially encased composite columns [14]. Patel et al. considered the influences of local buckling and proposed a fiber model to analyze CFST beam columns [15]. On the other hand, some structural measurements were proposed to resist local buckling in previous studies, such as setting straight ribs [16], tensile sheets [17], longitudinal and transverse stiffeners [18,19], binding bars [20], angle braces, and other kinds of buckling restrained braces [21,22]. Such measurements can improve the effect of steel tubes on confining concrete, but also result in construction operation difficulties, like the increase of welding workload and a decrease in construction quality. Therefore, some kind of new method needs to be explored to resolve some of these mentioned problems.

Here, longitudinal steel bars were set as stiffeners in the tube of square thin-walled CFST columns and spot welding was used to fix the steel bars onto the tubes, which were proposed as a new structural measure in this paper. Compared with some existing steel-plate stiffeners (Figure 1), the steel-bar stiffeners are simpler and more convenient for construction. In addition, steel bars have certain longitudinal rigidity and can be connected to the steel-pipe wall by spot welding. Using the spot-welding method can simplify the construction process and reduce the workload of welding significantly as well. To test the effect of such structural measures and their feasibility in practical projects, an experimental study was conducted in this paper on the compression behaviors of square thin-walled CFST columns with steel-bar stiffeners inside the tube. Several setting methods of the steel-bar stiffeners were compared and analyzed on their improving effects on the mechanical performance of stub columns through static-loading experiments.

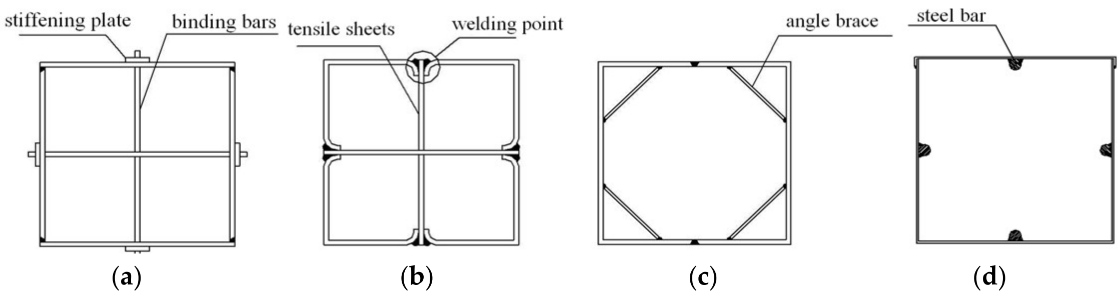


**Figure 1.** Comparison of existing stiffeners and steel-bar stiffeners. (**a**) Binding bar; (**b**) tensile sheet; (**c**) angle brace; (**d**) steel bar.

## 2. Experimental Program

### 2.1. Test Specimens

Six column specimens were fabricated in the test. The square tubes of the column specimens were made of Q235 cold-rolled steel sheets with a thickness of 2 mm. The section width of a square tube was 200 mm. To unify the stress of the column sections under the axial static loads applied at the end of columns, steel sheets of 250 × 250 × 6 mm were welded on both ends of the column specimens. The specimen details are shown in Figure 2.

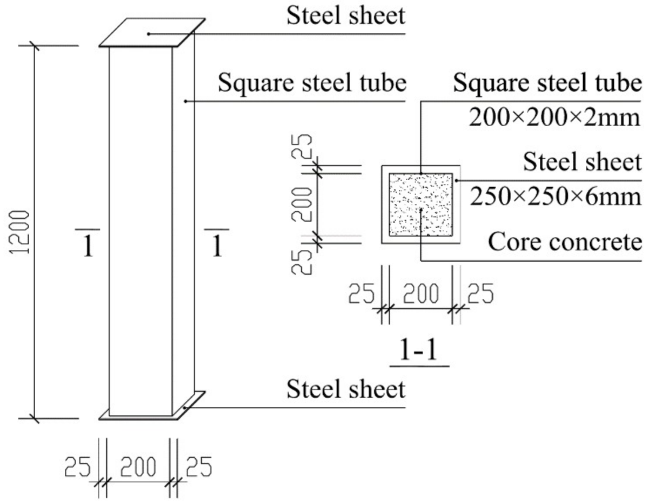


**Figure 2.** Details of column specimen.

The diameter of steel bars was determined according to the requirements of the minimum inertial moment of stiffeners. HPB235 steel bars were used to make the stiffeners of the specimens for welding convenience and better ductility.

The specimen plan is shown in Table 1. There are two thin-walled CFST columns with steel-bar stiffeners inside the tube, two thin-walled CFST columns with steel-bar stiffeners outside the tube, one thin-walled CFST column without any stiffeners inside, and one steel tubular column without concrete and stiffeners inside the tube. The section details of the specimens are shown in Figure 3.

**Table 1.** Specimen plan.

| Column Number | Stiffener Setting | Concrete Setting | Column Height (mm) | Column Width (mm) | Tube Thickness (mm) | Steel-Bar Diameter (mm) | Cross-Section Area Ratio of Steel to Column |
|---|---|---|---|---|---|---|---|
| C1 | Empty tube | No concrete | 1200 | 200 | 2 | - | 100% |
| C2 | No stiffeners | Concrete-filled | 1200 | 200 | 2 | - | 3.96% |
| C3 | Steel-bar stiffener inside tube | Concrete-filled | 1200 | 200 | 2 | 12 mm | 5.07% |
| C4 | Steel-bar stiffener inside tube | Concrete-filled | 1200 | 200 | 2 | 16 mm | 5.91% |
| C5 | Steel-bar stiffener outside tube | Concrete-filled | 1200 | 200 | 2 | 12 mm | 5.07% |
| C6 | Steel-bar stiffener outside tube | Concrete-filled | 1200 | 200 | 2 | 16 mm | 5.91% |

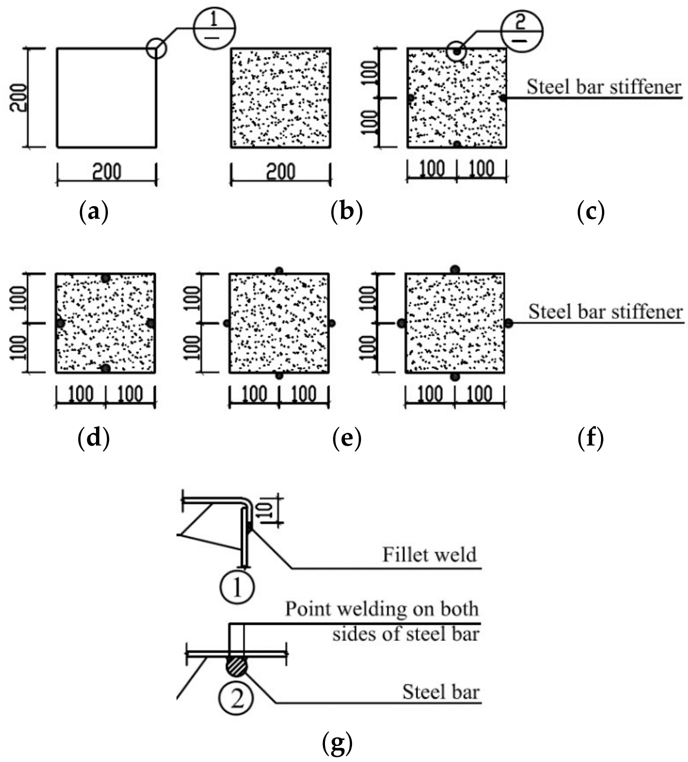


**Figure 3.** Section details of the specimens. (**a**) C1; (**b**) C2; (**c**) C3; (**d**) C4; (**e**) C5; (**f**) C6; (**g**) connection details.

### 2.2. Specimen Fabrication

The square thin-walled steel tube was made of two parts, including a U-shaped steel plate and a flat steel plate. The square steel tube was formed by welding those two parts together. The welding method is shown in Figure 3g.

For the columns with the steel-bar stiffeners inside the tube, the bars were fixed on the steel plates by spot welding before welding the two parts of plates together. The distance of two welding spots was set to be 10 mm along the bars. The cover plate was then welded onto one of the column ends. For the columns with the steel-bar stiffeners outside the tube, the two parts of steel plates were first welded together to form the square tube. The cover plate was then welded onto one of the column ends. The steel bars were finally fixed onto the plates by spot welding.

When casting concrete into the square steel tube, the tube was placed on the ground vertically and the concrete was poured into the tube layer by layer. A vibrator with a diameter of 50 mm was used in the concrete casting to densify the concrete. At the final casting, the top of the concrete was made to be flush with the top of the steel tube. After two weeks of curing, there was some longitudinal shrinkage in the concrete. So, cement mortar was used to again make the filler top flush with the top of steel tube. Then the cover steel plate was used to close the top of the square steel tube by welding. For each column, a group of three cubic concrete specimens were made and cured to test the mechanical properties of the concrete in the steel tube.

### 2.3. Materials Properties

The mechanical properties of steel plates and steel bars were tested through tensile experiments according to Chinese code GB/T 228.1-2010 [23]. The mechanical properties of concrete were tested through compressive experiments according to Chinese code GB/T 50081-2002 [24]. The tested properties of the steel materials and concrete are shown in Tables 2 and 3, respectively.

**Table 2.** Properties of steel materials.

| Type | Yield Strength ($N{\cdot}mm^{-2}$) | Ultimate Strength ($N{\cdot}mm^{-2}$) | Elastic Modulus ($N{\cdot}mm^{-2}$) |
|---|---|---|---|
| Steel tube | 243.0 | 368.5 | $1.82 \times 10^5$ |
| Steel bar | 231.3 | 355.3 | $1.97 \times 10^5$ |

**Table 3.** Properties of concrete.

| Type | Cube Compressive Strength ($N{\cdot}mm^{-2}$) | Axial Compressive Strength ($N{\cdot}mm^{-2}$) | Elastic Modulus ($N{\cdot}mm^{-2}$) |
|---|---|---|---|
| Core concrete | 24.5 | 16.4 | $2.77 \times 10^4$ |

### *2.4. Loading and Measurement*

Static-loading experiments were conducted using a 5000 kN hydraulic pressure-testing machine, which is shown in Figure 4. The static pressure load was applied onto the column specimens step by step. At the beginning, each load step was 1/10 of the ultimate load of the column, and then adjusted to 1/20 of the ultimate load of the column when close to the ultimate load. The load and displacement of column top were detected by the data-collection system and recorded in a computer. With the load being applied step by step, the relationship of load and longitudinal displacement was planned by the computer, which could be used to monitor the experimental process and determine the yield-load and ultimate-load values.

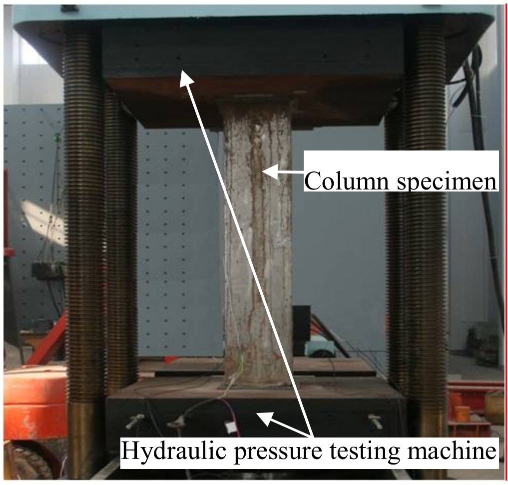


**Figure 4.** 5000 kN hydraulic pressure-testing machine.

## 3. Test Results

### *3.1. Failure Mode*

The failure modes of all the specimens are shown in Figure 5. For column C1, with no concrete inside the steel tube, concave local buckling of the steel plate occurred in one side of the square steel tube and convex local buckling of the steel plate occurred in the opposite side.

For column C2, with concrete but no stiffeners inside the steel tube, three buckling waves were formed in the middle of the steel tube. Although local buckling occurred in the thin-walled steel tube, the failure mode of this column was shear failure due to the support of the concrete inside the tubing.

For columns C3 and C4, with both concrete and steel-bar stiffeners inside the steel tube, shear failure was found as the main failure mode. Local buckling occurred in the upper areas of the tube and the thin plate of the square tube was pushed out by the steel bars inside.

For columns C5 and C6, which had concrete inside and steel-bar stiffeners outside the steel tube, shear failure was observed as the main failure mode as well. Local buckling occurred in the areas close to the end of the tube. The buckling waves of steel-bar stiffeners were the same as the waves of the steel plates in C5 for the smaller stiffness of the steel bars with a 12 mm diameter. The welding points between the bars and the plates were almost undamaged. Some buckling waves of the steel-bar stiffeners in C6 were bigger than the steel plates for the larger stiffness of the bars with a 16 mm diameter. The welding points in the big buckling waves were almost damaged.

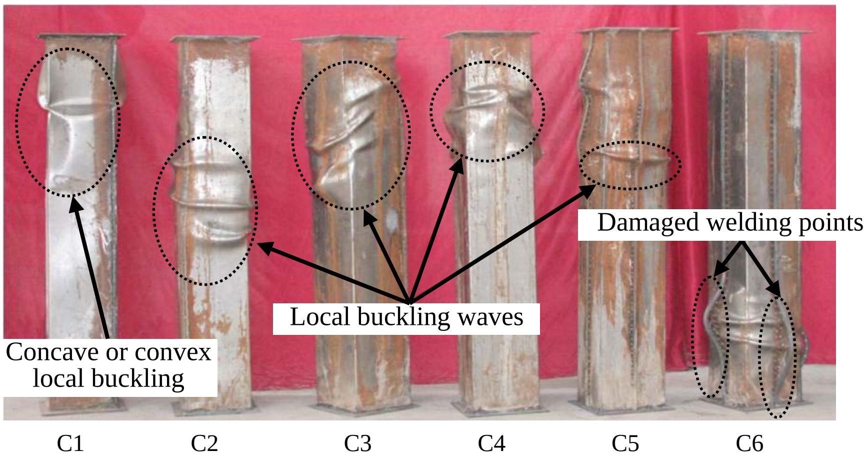


**Figure 5.** Failure modes of specimens.

### *3.2. Load–Displacement Relationship*

The load–displacement relationship curves of the six column specimens are shown in Figure 6. Three stages were observed in Figure 6. In the first stage, the displacement was small and proportionally increased with the load. Columns were still in the range of elasticity under the test load. However, in the second stage, the value of loads began to decrease, with displacement increasing after achieving the ultimate load. The higher the ultimate load was, the more rapidly the load decreased. When it came to the ultimate load, the displacement of C3 was the biggest among all the specimens, 10.1 mm, and the displacement of C6 was the smallest, 4.6 mm. In the last stage, the load tended to stabilize or increase a little, while displacement increased rapidly leading to the final damage of the columns. It has been observed that the displacement of the columns ranged from 20 to 40 mm as the loads stabilized.

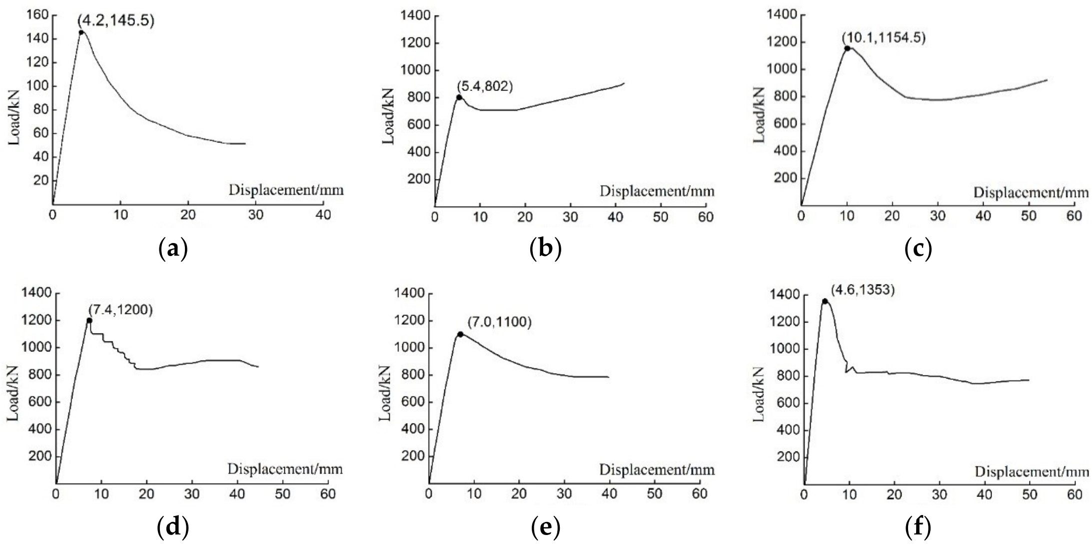


**Figure 6.** Load–displacement relationship curves of column specimens. (**a**) C1; (**b**) C2; (**c**) C3; (**d**) C4; (**e**) C5; (**f**) C6.

The ultimate load of C2, with a value of 802 kN, was significantly larger as compared to C1. Columns with stiffeners, meanwhile, achieved an even larger ultimate load than C2, ranging from

1100 to 1353 kN. It can also be observed that C6, with steel-bar stiffeners outside the tube, reached the highest ultimate load among the columns with a value of 1353 kN. It can be concluded that the ultimate load and maximum displacement of the concrete-filled columns with stiffeners were much larger than the columns without any stiffeners, which proved that the stiffeners were very useful in improving the mechanical performance of the square thin-walled CFST columns.

### *3.3. Ultimate Load*

In order to study the effect of steel-bar stiffeners on the axial bearing capacity of the columns, nominal bearing capacity was used in this study. Nominal bearing capacity means that the axial bearing capacity of a square thin-walled CFST column was assumed to be composed of three parts without considering the confinement effect on the core concrete provided by the steel tube. The first part is the capacity of the concrete inside the tube, the second one is the capacity of the steel tube, and the last part is the capacity of the stiffeners. The formula used to calculate the nominal bearing capacity of the columns is shown in Equation (1):

$$N_0 = f_c \times A_c + f_{yt} \times A_{st} + f_{ys} \times A_{ss} \quad (1)$$

where $N_0$ is the nominal bearing capacity of the column, kN; $f_c$ is the strength of concrete inside the steel tube, N/mm$^2$; $A_c$ is the cross-section area of the concrete, mm$^2$; $f_{yt}$ is the strength of the steel tube, N/mm$^2$; $A_{st}$ is the cross-section area of the steel tube, mm$^2$; $f_{ys}$ is the strength of the steel-bar stiffener, N/mm$^2$; and $A_{ss}$ is the cross-section area of the steel-bar stiffener, mm$^2$.

The axial bearing capacities of the eight column specimens obtained from the static-loading tests were compared with the nominal bearing capacities calculated according to Equation (1), which is shown in Table 4. In Table 4, $N_{ue}$ is the actual bearing capacity of the columns obtained from the tests.

**Table 4.** Comparison of axial bearing capacity of columns.

| Column Number | $A_{ss}$ (mm$^2$) | $N_{ue}$ (kN) | $N_0$ (kN) | $N_{ue}/N_0$ |
|---|---|---|---|---|
| C1 | - | 145.0 | 384.9 | 0.377 |
| C2 | - | 802.0 | 1014.9 | 0.790 |
| C3 | 452.4 | 1154.5 | 1119.6 | 1.031 |
| C4 | 804.2 | 1200.0 | 1200.9 | 0.999 |
| C5 | 452.4 | 1100.0 | 1119.6 | 0.983 |
| C6 | 804.2 | 1353.0 | 1200.9 | 1.127 |

Table 4 shows that the $N_{ue}/N_0$ of C1 s only 0.377. Because of this, local buckling in the thin steel plate of the square tube led to an unstable failure of the column before the steel reached yield strength. As a result, the actual bearing capacity of the column was much lower than the nominal capacity.

For C2, the supply to the tube from the concrete inside significantly increased the bearing capacity of the column. However, due to the high ratio of the cross-section width of the square tube to tube-wall thickness, local buckling occurred earlier leading to a premature failure of the column. Thus, the actual bearing capacity of the column was still lower than the nominal capacity.

For the column specimens with stiffeners inside or outside the tube, bearing capacities were increased significantly as compared with C2, and especially the bearing capacity of C6, with a 16 mm diameter steel bar outside the tube, which increased by 68.7% compared with C2. The ratios of $N_{ue}/N_0$ of these columns were all around 1.0, and the ratio of C6 even reached 1.127. Such observations verified that the steel-bar stiffeners were able to provide effective support to delay the local buckling that occurred in the steel plate of the tube, which improved the confinement effect from the steel tube on the core concrete and made better use of the steel's material properties.

The actual bearing capacity of C3 with 12 mm diameter steel bars inside was higher than that of C5 with the same-diameter bars outside the tube. This phenomenon can be explained as follows. When the 12 mm diameter steel bars were used as stiffeners, the cross-section area ratio of steel to column increased from 3.96% to 5.07% (Table 1). This increase can lead to the increase of the stiffness of the steel tube, and can provide support to resist local buckling. But when the increase of the steel cross-section area ratio was 1.11%, the support provided by the steel-bar stiffeners was still not sufficient. So when these steel bars were used outside of the steel tube as specimen C5, they could not give sufficient support to the steel tube to resist local buckling, although the total area of the column section was bigger. When the steel bars were used inside of the steel tube as specimen C3, the core concrete inside the tube could provide good confinement to the steel bars. Thus, the stiffness of the bars could be increased and better support could be provided to the steel tube to resist local buckling. Therefore, the bearing capacity of C3 was higher than that of C5.

Meanwhile, the actual bearing capacity of C6 with 16 mm diameter steel bars outside was higher than that of C4 with the same diameter bars inside the tube. This condition was different to that of C3 and C5, which can be explained as follows. When the 16 mm diameter steel bars were used as stiffeners, the cross-section area ratio of steel to column increased from 3.96% to 5.91% (Table 1). This 1.95% increase of the steel cross-section area ratio could lead to sufficient stiffness increase in the steel tube, and provide better support to the steel tube to resist local buckling regardless of being inside or outside the tube. Thus, when they were put outside the tube, the total area of column section to bear the load was larger than that of the column with the steel bars put inside the tube. Therefore, the bearing capacity of C6 was higher than C4.

From the above analysis, it can be seen that steel-bar stiffeners can effectively improve the bearing capacity of square thin-walled CFST columns. In addition, compared with the traditional way of increasing wall thickness, the steel-bar stiffener has a better effect on improving the bearing capacity of the column. Taking C4 as an example, when four 16 mm steel bars were used, the increase of steel content was equivalent to increasing the wall thickness of the steel pipe from 2 mm to 3 mm. However, it is calculated that, when the steel-pipe wall thickness is 3 mm, the increase of the bearing capacity of the columns is about 15% [25] relative to a wall thickness of 2 mm, while the increase is about 50% after steel-bar stiffeners are used.

### 3.4. Ductility

To study the effect of steel-bar stiffeners on the ductility of columns under axial pressure load, ductility coefficients of the columns were calculated in this paper. The formula of ductility coefficient is shown in Equation (2):

$$DI = \Delta_{max}/\Delta_y \tag{2}$$

In Equation (2), $DI$ is the ductility coefficient; $\Delta_{max}$ is the maximum axial displacement of the column top, which was assumed to be taken when the load dropped to 85% of the ultimate load in this paper; $\Delta_y$ is the yielding displacement of the column top, which was assumed to be taken when the load increased to 75% of the ultimate load in this paper [26].

According to Equation (2), the comparison of the ductility of all column specimens except C1 is shown in Table 5.

**Table 5.** Comparison of ductility of columns.

| Column Number | $\Delta_y$/mm | $\Delta_{max}$/mm | DI |
|---|---|---|---|
| C2 | 5.1 | 17.5 | 3.43 |
| C3 | 7.2 | 14.5 | 2.01 |
| C4 | 5.0 | 10.5 | 2.10 |
| C5 | 4.4 | 14.1 | 3.20 |
| C6 | 3.5 | 8.1 | 2.31 |

It can be seen from Table 5 that the ductility of the column with steel-bar stiffeners was lower than the column (C2) without any steel-bar stiffeners. In the columns (C3~C6) with stiffeners, the values of $DI$ ranged from 2.01 to 3.20, while the value of the $DI$ of C2 was 3.43. It proved that steel-bar stiffeners could decrease the ductility of these columns. The reason is that the steel bars significantly increased the bearing capacity of the columns, but when these steel bars yielded, bearing capacity rapidly decreased. Then, ductility decreased too.

In the columns with steel-bar stiffeners inside the tube (C3 and C4), the difference in steel-bar diameter made little difference in column ductility. The ductility of this kind of columns was lower than in the columns with stiffeners outside the tube because the constraint from the core concrete and steel tube lowered the deformation capacity of the steel bars.

In the columns with steel-bar stiffeners placed outside the tube (C5 and C6), the *DI* value of C5 was 3.20, while that of C6 was 2.31. It proved that a higher cross-section area ratio of steel to column can lead to lower deformation capacity for the column, while a lower steel-section area ratio can result in higher deformation capacity.

### 3.5. Local Buckling

Under axial loads, square thin-walled CFST columns are easier to have local buckling occur than round columns, especially when the ratio of cross-section width of the tube to tube-wall thickness is high. To study the effect of steel-bar stiffeners on delaying or avoiding local buckling, the loads when local buckling was observed to be occurred, called local-buckling load in the paper, were compared in Table 6. In Table 6, $N_u$ is ultimate load; $N_q$ is the local-buckling load; $N_{qi}/N_{q2}$ is the ratio of local-buckling load of other columns to the load of column C2.

**Table 6.** Comparison of local-buckling load of columns.

| Column Number | $N_u$ (kN) | $N_q$ (kN) | $N_q/N_u$ | $N_{qi}/N_{q2}$ |
|---|---|---|---|---|
| C1 | 145.5 | 120.0 | 0.825 | 0.194 |
| C2 | 802.0 | 620.0 | 0.773 | 1.000 |
| C3 | 1154.5 | 700.0 | 0.606 | 1.129 |
| C4 | 1200.0 | 820.0 | 0.683 | 1.323 |
| C5 | 1100.0 | 760.0 | 0.691 | 1.226 |
| C6 | 1353.0 | 880.0 | 0.650 | 1.419 |

It can be seen from Table 6 that the $N_q$ of every column is less than $N_u$, which proved that all the columns had local buckling before they damaged under axial loads.

Comparing the local-buckling loads, C2 was much higher than C1, which means that the concrete inside provided significant help in delaying local buckling. As to the columns with steel-bar stiffeners inside or outside the tube, the local-buckling loads were obviously higher than C2, especially C6, with 16 mm diameter steel bars outside the tube, which was higher than C2 by 41.9%. It can be concluded that steel-bar stiffeners are effective in delaying local buckling.

## 4. Summary and Conclusions

Through static-loading tests and analysis, the mechanical properties of square thin-walled CFST columns with steel-bar stiffeners were studied. The effect of different structural measures was compared. The following conclusions were drawn:

(1) When steel-bar stiffeners are placed inside or outside the steel tube of square thin-walled CFST columns, they can effectively delay local buckling in thin steel tubes. Higher local-buckling loads and ultimate bearing capacity of the columns can be achieved as well. However, the ductility of the columns decreased.

(2) When the increase of the cross-section area ratio of steel to column is 1.11%, steel-bar stiffeners can work better when placed inside the steel tube and obtain higher bearing capacity of columns, because of the constraint effect of core concrete. When the increase of the cross-section area ratio of steel to column is 1.95%, steel-bar stiffeners should be placed outside the steel tube to enlarge the cross-section area of the column and obtain higher bearing capacity.

(3) A higher cross-section area ratio of steel to column can lead to lower deformation capacity for the column, while a lower steel-section area ratio can result in higher deformation capacity.

(4) The structural measures of using steel bars as stiffeners and using spot welding to fix the steel bars onto the tube to strengthen square thin-walled CFST columns are effective and feasible, which can delay local buckling in the tube, increase the bearing capacity of the column, and save construction costs.

**Author Contributions:** Z.Y. and C.X. designed the experiment procedures. Z.Y. performed the experiments. Z.Y. and C.X. analyzed the data. Z.Y. wrote the original draft of this paper. C.X. gave some suggestions to polish the paper.

**Funding:** The work was financially supported by the National Natural Science Foundation of China (Project code: 51678457), the Scientific Research Key Project Fund of Ministry of Education of Hubei Province (Project code: D20171106), and the Research Foundation of Wuhan Construction Committee (Project code: 201820). Their support is gratefully acknowledged.

**Conflicts of Interest:** The authors declare no conflict of interest.

## References

1. Ahmad, F. Local Buckling Restraining Behavior of Concrete-Filled Steel Tubular Columns under Seismic Loads. Master's Thesis, University of North Dakota, Grand Forks, ND, USA, 2015.
2. Montuori, R.; Piluso, V. Analysis and modelling of CFT members: Moment curvature analysis. *Thin-Walled Struct.* **2015**, *86*, 157–166. [CrossRef]
3. Elchalakani, M.; Karrech, A.; Hassanein, M.F.; Yang, B. Plastic and yield slenderness limits for circular concrete filled tubes subjected to static pure bending. *Thin-Walled Struct.* **2016**, *109*, 50–64. [CrossRef]
4. Choi, I.R.; Chung, K.S.; Kim, C.S. Experimental study on rectangular CFT columns with different steel grades and thicknesses. *J. Constr. Steel Res.* **2017**, *130*, 109–119. [CrossRef]
5. Campiche, A.; Shakeel, S.; Macillo, V.; Terracciano, M.T.; Bucciero, B.; Pali, T.; Fiorino, L.; Landolfo, R. Seismic behaviour of sheathed CFS buildings: Shake table tests and numerical modelling. *Ing. Sism.* **2018**, *35*, 106–123.
6. Ghazijahani, T.G.; Jiao, H.; Holloway, D. Timber filled CFRP jacketed circular steel tubes under axial compression. *Constr. Build. Mater.* **2015**, *94*, 791–799. [CrossRef]
7. Ghazijahani, T.G.; Asce, S.M.; Jiao, H.; Holloway, D. Concrete-Filled Circular Steel Tubes with a Timber Infill under Axial Compression. *J. Struct. Eng.* **2017**, *143*, 1–29. [CrossRef]
8. Ding, F.X.; Liu, J.; Liu, X.M.; Yu, Z.W.; Li, D.W. Mechanical behavior of circular and square concrete filled steel tube stub columns under local compression. *J. Thin-Walled Struct.* **2015**, *94*, 155–166. [CrossRef]
9. Uy, B.; Bradford, M.A. Elastic local buckling of steel plates in composite steel-concrete members. *Eng. Struct.* **1996**, *18*, 193–200. [CrossRef]
10. Schnabl, S.; Jelenić, G.; Planinc, I. Analytical buckling of slender circular concrete-filled steel tubular columns with compliant interfaces. *J. Constr. Steel Res.* **2015**, *115*, 252–262. [CrossRef]
11. Thai, H.T.; Uy, B.; Khan, M. A modified stress-strain model accounting for the local buckling of thin-walled stub columns under axial compression. *J. Constr. Steel Res.* **2015**, *111*, 57–69. [CrossRef]
12. Dundu, M. Column buckling tests of hot-rolled concrete filled square hollow sections of mild to high strength steel. *J. Eng. Struct.* **2016**, *127*, 73–85. [CrossRef]
13. Long, Y.L.; Wan, J.; Cai, J. Theoretical study on local buckling of rectangular CFT columns under eccentric compression. *J. Constr. Steel Res.* **2016**, *120*, 70–80. [CrossRef]
14. Song, Y.C.; Wang, R.P.; Li, J. Local and post-local buckling behavior of welded steel shapes in partially encased composite columns. *J. Thin-Walled Struct.* **2016**, *108*, 93–108. [CrossRef]
15. Patel, V.I.; Liang, Q.Q.; Hadi, M.N.S. Nonlinear analysis of biaxially loaded rectangular concrete-filled stainless steel tubular slender beam-columns. *Eng. Struct.* **2017**, *140*, 120–133. [CrossRef]
16. Zhang, Y.C.; Chen, Y. Experimental study and finite element analysis of square stub columns with straight ribs of concrete-filled thin-walled steel tube. *J. Build. Struct.* **2006**, *27*, 16–22. (In Chinese)
17. Chen, Y.; Zhang, Y.C. Experimental study and finite element analysis of square stub columns with tensile sheets of concrete–filled thin–walled steel tube. *J. Build. Struct.* **2006**, *27*, 23–29. (In Chinese)

18. Zhu, C.A.; Xu, C.X. Design and Selection of constructional measures to Restrict Local Buckling of Concrete Filled Thin-Walled Square Steel Tube Columns. *J. Yangtze Univ. (Nat. Sci. Ed.) Sci. Eng. V* **2008**, *5*, 378–380. (In Chinese)
19. Li, L.Z.; Jiang, C.J.; Jia, L.J.; Lu, Z.D. Local buckling of bolted steel plates with different stiffener configuration. *Eng. Struct.* **2016**, *119*, 186–197. [CrossRef]
20. Wang, Y.T.; Cai, J.; Long, Y.L.; Chen, Q.J. Bearing behavior under compression and bending of concrete-filled square steel tubular columns with confined bars. *Ind. Constr.* **2016**, *46*, 142–148. (In Chinese)
21. Guo, Y.L.; Zhang, B.H.; Jiang, Z.Q.; Chen, H. Critical load and application of core-separated buckling-restrained braces. *J. Constr. Steel Res.* **2015**, *106*, 1–10. [CrossRef]
22. Talebi, E.; Tahir Md, M.; Zahmatkesh, F.; Kueh, B.H.A. Comparative study on the behavior of Buckling Restrained Braced frames at fire. *J. Constr. Steel Res.* **2014**, *102*, 1–12. [CrossRef]
23. GB/T 228.1-2010. *Metallic Materials–Tensile Testing-Part 1: Method of Test at Room Temperature*; Ministry of Housing and Urban-Rural Development of the People's Republic of China (MOHURD): Beijing, China, 2010. (In Chinese)
24. GB/T 50081-2002. *Standard for Test Method of Mechanical Properties on Ordinary Concrete*; Ministry of Housing and Urban-Rural Development of the People's Republic of China (MOHURD): Beijing, China, 2002. (In Chinese)
25. GB 50936-2014. *Technical Code for Concrete Filled Steel Tubular Structures*; Ministry of Housing and Urban-Rural Development of the People's Republic of China (MOHURD): Beijing, China, 2014. (In Chinese)
26. Han, L.H.; Zhao, X.L. Test and calculations for hollow structural steel (HSS) stub columns filled with self-consolidating concrete (SCC). *J. Constr. Steel Res.* **2005**, *61*, 1241–1269. [CrossRef]